

# Resistance Characteristic of High-speed Unstaggered Pentamaran Model with Variations of Symmetric and Asymmetric Hull Configurations

Yanuar<sup>1</sup> · Ibadurrahman<sup>1</sup> · R. Muhammad Arif<sup>1</sup> · D. P. Muhamad Ryan<sup>1</sup>

Received: 22 November 2018 / Accepted: 6 June 2019 / Published online: 7 January 2020  
© Harbin Engineering University and Springer-Verlag GmbH Germany, part of Springer Nature 2020

## Abstract

Pentamaran, a vessel with five hulls, can be an alternative for high-speed vessels due to its advantages, for instance, its excellent stability and seakeeping performance and broader deck space than an equivalent monohull with the same displacement. The destructive interference between the system of waves produced by the vessel's hulls might benefit the reduction of power consumption. This study investigated a Wigley hull form pentamaran model with five asymmetric and symmetric hull configurations and three variations of hull separation. The ship model was towed in conditions of fixed towing and calm water with Froude numbers ( $Fr$ ) ranging from 0.55 to 1.00. A resistance analysis had been carried out to ensure proper comparison between the asymmetric and symmetric hull configurations. Results showed that total resistance coefficient of the asymmetries created different properties from the symmetries, that is, symmetries produced steadier trends than asymmetries. The hull separation variation caused a slight alteration in the total resistant coefficient (in magnitude) under the same configuration. Although not a single configuration outperformed the others in the entire range of  $Fr$ , three configurations were noteworthy as optimum models based on their  $Fr$  range. Moreover, a configuration of asymmetric hull with  $S/L = 0.22$  could generate a constant destructive interference throughout the investigated  $Fr$  range.

**Keywords** Unstaggered pentamaran · Asymmetric hull · Symmetric hull · Interference factor · Hull separation

## 1 Introduction

Multihull is an alternative hull design for high-speed vessels and provides certain advantages compared with a conventional monohull vessel, for instance, having a larger deck area and providing better static and dynamic stabilities. Multihulls can

serve many purposes and are commonly operated in the high-speed range (Hajiabadi et al., 2018).

Multihulls can be configured in various configurations, with each configuration having distinctive resistance properties. According to the resistance aspect, one factor is needed to achieve an optimum body of multihull configuration: the wave interactions between individual hulls. Wave interaction is associated directly with wave-making resistance and total resistance. Insel and Molland (1992), Zaghi et al. (2011), and Broglia et al. (2014) have shown that resistance and wave interference characteristics of a catamaran rely on the separation distance between the demihulls; a stronger interference effect in wave-making resistance results from a smaller separation distance.

Another multihull vessel, the trimaran, consists of one main hull and two symmetric or asymmetric sidehulls, which are generally shorter. These shorter sidehulls, which may also be called outriggers, are positioned on both sides of the main hull. As sidehulls are essential to the overall layout and structural design of the vessel, their configuration should be decided in the early design phase; this decision will impact the

## Article Highlights

- In order for multihull resistance to be detected whether is more efficient than monohull or not, a comparison with non-interference multihull must be conducted.
- The pentamaran model is towed in fixed trim-sinkage and calm water condition.
- Experimental data of five model configurations and three hull separation variations are presented and compared with each other.
- The performance of each model configuration is studied and seen dependent on Froude number range and hull separation.

✉ Yanuar  
yanuar@eng.ui.ac.id

<sup>1</sup> Department of Mechanical Engineering, Universitas Indonesia, Jakarta 16424, Indonesia

hydrodynamic performance of the vessel (Doctors and Scrase, 2003; Wu et al., 2011). Previous numerical and experimental studies on trimaran by Su et al. (2014) and Yu et al. (2015) have shown that this vessel performance could be improved by adjusting the vessel configuration depending on its service speed; thus, an optimum configuration may be achieved. Hafez and El-Kot (2011) and Yanuar et al. (2013) concluded that an optimal configuration might experience a destructive interference between the waves generated by each hull; this phenomenon will subsequently reduce the total resistance of the vessel.

These performance-affected elements also influence other multihull vessels, such as tetramaran and quadramaran. Tuck and Lazaukas (1998) had tested multiple models of multihull ship configurations; from their investigation, sidehull positional variation considerably influenced the interference resistance for any multihull configuration, including the tetramaran and quadramaran configurations, agreeing well with the experimental results obtained by Yanuar et al. (2016).

A vessel with five hulls, the pentamaran, exhibits excellent stability and seakeeping performance and broader deck space than an equivalent monohull with the same displacement (Dudson and Gee, 2001; Ikeda et al., 2005). Several researchers had conducted investigations on pentamaran vessels. Tarafder et al. (2013) showed that the wave interference was minimum under a Froude number ( $Fr$ ) greater than 0.8, and hence, the wave-making resistance could be reduced. Yanuar et al. (2017a) demonstrated that each configuration induced a different resistance characteristic depending on the  $Fr$  range and hull separation; their results confirmed that a configuration with smaller hull separation indicates a higher interference resistance compared with other configurations.

Studies on pentamaran resistance characteristics with regard to the interference effect remain unfinished as this type of vessel has many possible configurations. For this reason, the latest investigations on pentamaran vessel focused on inspecting new configurations to obtain an optimum resistance characteristic at a certain speed range. Further research may give a clear explanation about the interference phenomenon, which is associated with vessel performance.

Investigation on a new configuration of a pentamaran vessel, which includes asymmetrical hulls, is well underway and serves as the objective of this paper. The scope of this study focuses on the characteristic of model resistance, along with the interference factor (IF) in a specific  $Fr$  range, that is, from medium to high. As interference phenomenon affects both wave-making resistance and viscous resistance of a multihull vessel, in this study, only these resistances were considered as important among the resistance components.

## 2 Experimental Setup

This study investigated a pentamaran model with a variety of asymmetric and symmetric hull configurations combined with a range of hull separation. The model was arranged from two identical asymmetrical hulls and three identical symmetrical hulls. Both asymmetric hulls were placed in either the inner side or outer side of the main hull and configured in either the inboard or outboard position. Figure 1 shows the line plan of the pentamaran model with Wigley hull form.

The configuration of individual hulls determines the main geometry of a multihull vessel.  $L_{oa}$  of the model refers to the hull length. The beam of a pentamaran is affected by both spaces between the main hull and inner sidehull and between inner and outer sidehulls. In this investigation, every space between hulls had the same distance, and three space variations were applied. Thus, the beam measurement of the pentamaran model varied. Table 1 presents the characteristics of the individual hull model.

Figure 2 depicts the model's main geometry with the reference system. The  $S$  notation denotes a distance from a hull centerplane to another hull centerplane. Furthermore, the examined model showed no variation in longitudinal distance (hull stagger). Therefore, the model had a constant length in all configurations. Thereby, when configurations were compared with each other, the  $Fr$  solely signified a function of the model speed.

In this study, the main hull was symmetric, and a pair of asymmetric and symmetric hulls were used alternately as side hulls. Moreover, an additional configuration of conventional

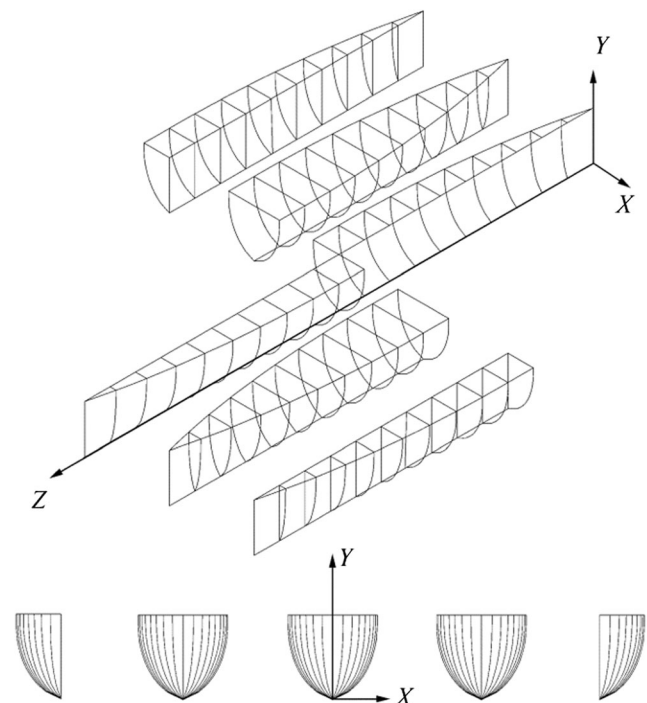


Fig. 1 Isometric line plan of the Wigley hull form of the ship model

**Table 1** Main dimensions of the individual hull model

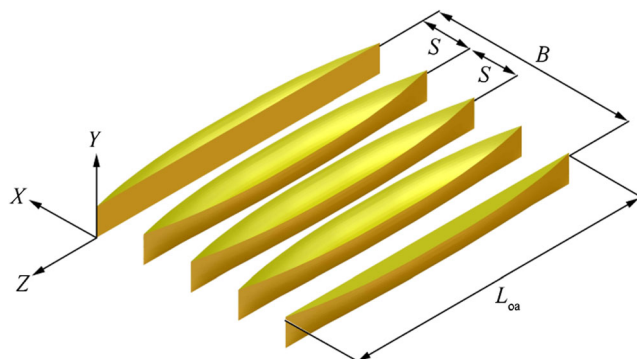
Properties	Symbol	Hull form	
		Asymmetric	Symmetric
Length (m)	$L_{oa}$	1.8	1.8
Beam (m)	$B$	0.09	0.18
Height (m)	$H$	0.17	0.17
Draft (m)	$T$	0.075	0.075
Block coefficient	$C_b$	0.361	0.361
Waterplane-area coefficient	$C_w$	0.523	0.523
Prismatic coefficient	$C_p$	0.699	0.699
Midship coefficient	$C_m$	0.517	0.517
Displacement (kg)	Disp	3.7	7.4
Wetted surface area (m <sup>2</sup> )	$S_a$	0.309	0.349

arrangement (all-symmetric hulls) was investigated for comparison and to analyze the asymmetric hull configurations; a pair of additional symmetric hulls substituted both asymmetric hulls. This study evaluated five main configurations, and a simple notation represented each one (see Fig. 3):

- A: outer inboard asymmetric hull position;
- B: outer outboard asymmetric hull position;
- C: inner inboard asymmetric hull position;
- D: inner outboard asymmetric hull position;
- E: symmetric hull position.

Each main configuration has three variations of hull-to-hull transverse space ( $S$ ), and Table 2 displays the variations in hull separation ( $S/L$  ratio) of the model.

Beam of configuration B exhibited a slight difference from the other configurations as its outer asymmetric sidehulls were oriented to the outward side. Given this condition, its beam was slightly narrower than that of the other configurations and twice as that of the asymmetric hull. Nevertheless, this slight difference in the models' beam presented no substantial concern as all models had the same length and hull separation.

**Fig. 2** Main geometry of the pentamaran model

Each configuration had been tested in a specified  $Fr$  range, that is, from medium to high. The ship model was towed in a water tank measuring 50-m long, 10-m wide, and 2-m deep in a fixed towing condition. The experimental setup consisted of some main instruments: a load cell transducer to measure total resistance of the running model, a set of data acquisition system to translate and record data from the load cell, and two laser probes to measure the model's speed. These probes were used in the model's speed measurement instead of the conventional method because the model was run up to the critical  $Fr$ . Excluding the model's speed measurement, the standard of the conducted vessel and procedures were determined under ITTC Recommended Procedures and Guidelines: Resistance Test (ITTC, 2011). Figure 4 illustrates the scheme of experimental setup.

The structural integrity of the pentamaran model was constructed rigidly to avoid structural bending or unevenness between individual hulls during towing. Four transverse frames were used as a separation adjustment system, and four additional longitudinal frame structures composed of steel L-bars were used to stiffen the model. Figure 5 illustrates the frame structure and adjustment system.

The experiment was performed in a calm water condition, where after every single test, a certain waiting time was engaged to maintain a steady calm water condition (Peng et al., 2004). The waiting time was strictly retained for a minimum of 15 min before starting the next test. A constant speed of the ship model had been ensured for every single test, in which the  $Fr$  was established from 0.55 to 0.1. Eleven data points were used to create a resistance trend on the observed  $Fr$  range for a single configuration (the total number of configuration is 15).

## 3 Result and Discussions

### 3.1 Resistance Analysis

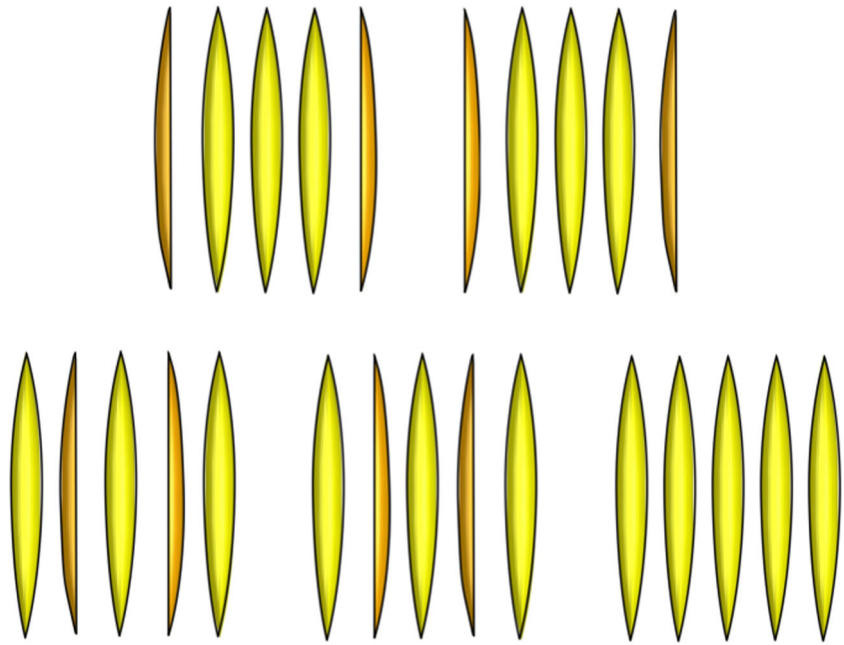
In this examination, resistance coefficients are used to introduce the data instead of its resistance values since they represent the characteristics of resistance and can be directly compared with each other (Yanuar et al., 2017b). Total resistance coefficient was calculated based on the experimental data, and according to ITTC 1957 is expressed as follows:

$$C_t = \frac{R_t}{0.5\rho(S_a)V^2} \quad (1)$$

$Fr$  is defined as follows:

$$Fr = \frac{V}{\sqrt{gL}} \quad (2)$$

where  $R_T$  refers to the measured total resistance of the model,  $\rho$  is water density,  $S_a$  denotes the total wetted surface area of

**Fig. 3** Main configuration of the pentamaran model

the model,  $L$  represents the model length, and  $V$  is the measured model speed. As the ship model was applied in a calm water condition, air resistance and correlation allowance were ignored in the current examination.

International Towing Tank Conference (ITTC, 2002) classified ship resistance in calm water into two components: viscous resistance and wave-making resistance, which is related to  $Fr$ . Viscous resistance is dominated by skin friction resistance, whereas wave-making resistance is influenced mainly by the hull form of the vessel and its speed (Wigley and Havelock, 1934).

A resultant wave generated from an individual speeding hull may be called a system of waves. Multihull system of waves is the sum of system waves of hulls, including any interaction between them.

When a system of waves interacts with another system of waves, two possibilities might occur: they merge and become a larger system of waves (constructive interference), or they diminish each other and become a weaker system of waves (destructive interference) or possibly terminate each other. A

multihull vessel experiences these wave interference phenomena, which are also known as hump and hollow. In the high  $Fr$  range, the proportion of wave-making resistance possibly exceeds that of skin friction resistance (Davidson, 1942). For this reason, interference issues must be analyzed from the design stage as they may reduce the total resistance of a multihull vessel or amplify it.

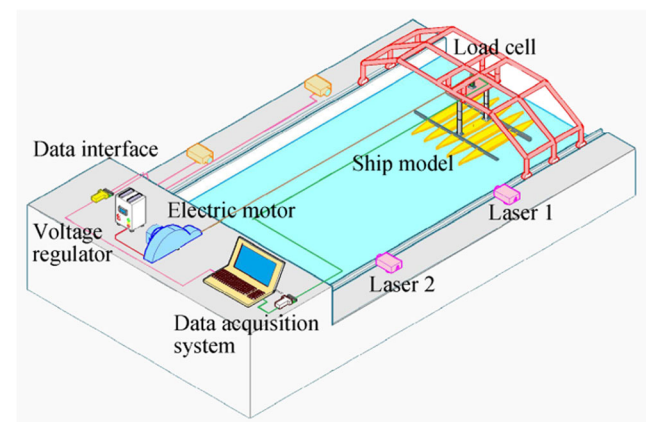
Although the components of multihull total resistance are intricate to examine, its interference phenomena can be detected with an experiment. The magnitude of interaction between the individual hulls of a pentamaran vessel is defined as an IF (Zaghi et al., 2011), which is calculated as follows:

$$IF = \frac{C_t^{(p)} - C_t^{(nonP)}}{C_t^{(nonP)}} \quad (3)$$

where  $C_T^{(P)}$  refers to the total resistance coefficient of the pentamaran model, and  $C_T^{(nonP)}$  denotes the total resistance

**Table 2** Hull separation of the pentamaran model

Asymmetric hull position	Symbol	$S/L$		
		1	2	3
Outer inboard	A	0.16	0.19	0.22
Outer outboard	B	0.16	0.19	0.22
Inner inboard	C	0.16	0.19	0.22
Inner outboard	D	0.16	0.19	0.22
-	E	0.16	0.19	0.22

**Fig. 4** Schematic of the experimental setup

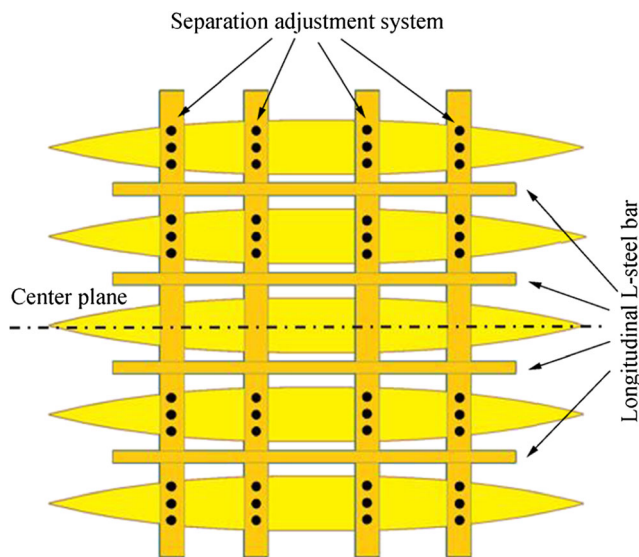


Fig. 5 Schematic of the frame structure and adjustment system

coefficient of non-interference pentamaran.

In the current study, the variations in model speed, configuration, and hull separation were used as parameters to investigate the characteristics of interference phenomena. A phenomenon may be deduced from the IF of the multihull vessel and determine whether it is a preferable effect (destructive interference) or not (constructive interference).

(4)

In the definition of  $C_T^{(nonP)}$  of the symmetric hull configuration, if the total resistance is five times the resistance of a single hull, then the wetted surface is also five times the surface of a single hull; this relation is expressed as follows:

$$R_t^{(nonP-sym)} = 5R_t^{(sym)} \quad (4)$$

Thus,  $C_T^{(nonP)}$  is the same as  $C_T$  of the single hull and must not be obtained by summation as each of them is referred to its own wetted surface. Instead, the following equation should be used:

$$C_t^{(nonP-sym)} = C_t^{(sym)} \quad (5)$$

However, the total resistance of pentamaran with asymmetric hull configuration differs from that with a symmetric hull configuration, and it can be defined as follows:

$$R_t^{(nonP-asym)} = 3R_t^{(sym)} + 2R_t^{(asym)} \quad (6)$$

Therefore, the total coefficient resistance of the asymmetric hull configuration is defined using the equation below:

$$C_t^{(nonP-asym)} = \frac{3C_t^{(sym)}S_a^{(sym)} + 2C_t^{(asym)}S_a^{(asym)}}{3S_a^{(sym)} + 2S_a^{(asym)}} \quad (7)$$

where  $C_t^{(sym)}$  and  $C_t^{(asym)}$  stand for total resistance coefficient of the individual symmetric and asymmetric hull forms,

respectively. The multihull IF has to be retained to the minimum if possible (Souto-Iglesias et al., 2012).

Figure 6 gives information about the total resistance coefficient of asymmetric and symmetric hulls and the non-interference pentamaran configurations. In general, the total resistance coefficient of both individual hulls decreased moderately, and the same results were observed for non-interference pentamaran. These trends were expectedly similar to the trend of Wigley hull form resistance. Trends of  $C_t^{(nonP-sym)}$  coincided with  $C_t^{(sym)}$  as they were equal.

In multihull analysis, according to resistance characteristics, unless the vessel operates in slow to medium speed, its wetted surface area influences the resistance more than its displacement. Although the asymmetric hull form has different properties compared with the symmetric form, in this paper, the asymmetric hull configuration could be analyzed and compared directly with the symmetric hull configuration. Although displacement of the symmetric hull is twice that of the asymmetric one, their wetted surface areas differed slightly. Figure 7 compares the wetted surface areas of the two forms of individual hulls and pentamaran configuration. The wetted surface area of the non-interference pentamaran equals that of the pentamaran with interference.

For further clarification, the difference in wetted surface area between the hull forms is calculated as follows:

$$\Delta S_a^{(ind)} = \frac{S_a^{(sym)} - S_a^{(asym)}}{S_a^{(sym)}} 100\% \quad (8)$$

$\Delta S_a^{(ind)}$  was about 11.4%. As for the non-interference pentamaran, the difference in wetted surface area between two hull form configurations is calculated by the following:

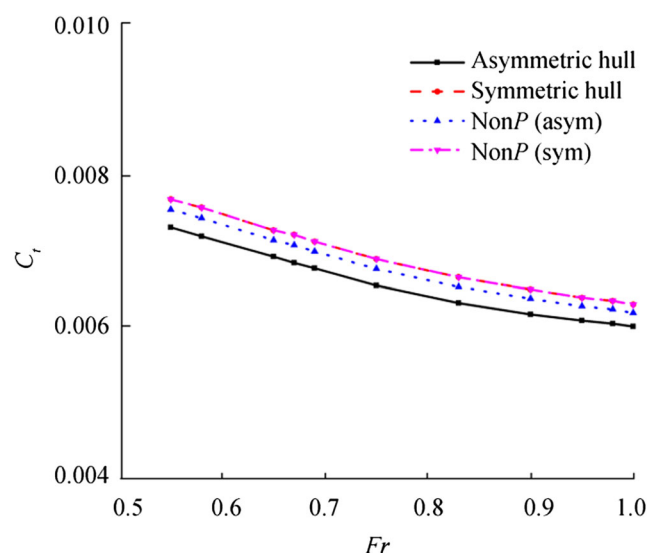
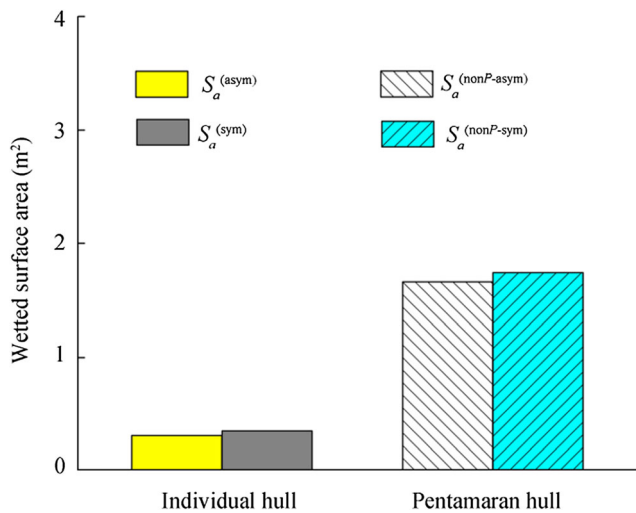


Fig. 6 Total resistance coefficient of individual hull and non-interference pentamaran





**Fig. 7** Wetted surface area of individual hull forms and pentamaran hull configuration

$$\Delta S_a^{(nonP)} = \frac{S_a^{(nonP-sym)} - S_a^{(nonP-asym)}}{S_a^{(nonP-sym)}} 100\% \quad (9)$$

$\Delta S_a^{(nonP)}$  was about 4.5%.

The wetted surface area influences the proportion of total resistance coefficient. However, this variable may only be applied for a vessel operating below the high-speed range as skin friction resistance is the dominant component of resistance at such range. To establish evidence of this condition, the average difference in total resistance coefficient between the individual hulls over the observed  $Fr$  range should be determined and calculated as follows:

$$\overline{\Delta C_t^{(ind)}} = \frac{1}{n} \sum_{i=1}^n \left( \frac{C_t^{(sym)} - C_t^{(asym)}}{C_t^{(sym)}} 100\% \right)_i \quad (10)$$

Hence,  $\overline{\Delta C_t^{(ind)}}$  was about 4.9%.

The average difference in total resistance coefficient between the non-interference pentamaran configurations over the observed  $Fr$  range should be determined to further support the evidence. This average can be calculated by taking the results from Eqs. (5) and (7), calculating the difference between the two configurations, and finally averaging the results over the  $Fr$  range, which can be expressed as follows:

$$\overline{\Delta C_t^{(nonP)}} = \frac{1}{n} \sum_{i=1}^n \left( \frac{C_t^{(nonP-sym)} - C_t^{(nonP-asym)}}{C_t^{(nonP-sym)}} 100\% \right)_i \quad (11)$$

The result was around 1.8%.

Figure 8 compares results of Eqs. (8), (9), (10), and (11). Based on the findings, the difference in wetted surface areas between the asymmetric and symmetric hulls can be neglected in the following resistance analysis as their difference is less

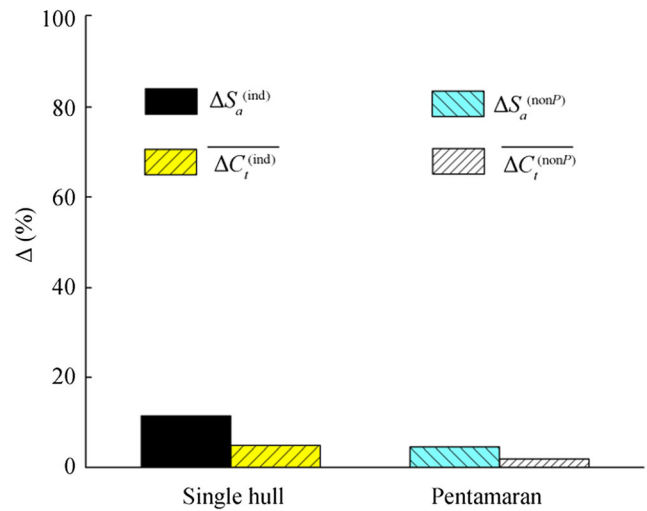


**Fig. 8**  $\Delta$  of wetted surface area and the average total resistance coefficient between individual hulls and non-interference pentamaran over the  $Fr$  range

than 2% of the total resistance coefficient of the pentamaran configuration. For such reason, symmetrical hull configurations may be compared with asymmetrical hull ones with confidence.

Wetted surface area relates to friction resistance. Based on the above results, however, as the difference in wetted surface area is neglected in the comparison, this investigation focused not on the viscous resistance, i.e., skin friction resistance, which possibly originates from the hull, but rather the other resistance component, that is, the wave-making resistance. Therefore, the difference between the resistance characteristics of the asymmetric and symmetric hull configurations is solely due to interference of their system of waves.

### 3.2 Total Resistance Coefficient

Figure 9 shows the total resistance coefficient of asymmetric hull configurations, where the asymmetric hulls were placed as outer sidehull (A and B) and with each featuring three variations of hull separation. From the starting  $Fr$ , their general trends rose and reached a peak point: configuration A was at  $Fr = 0.83$ , and configuration B was at  $Fr = 0.94$ .

From the initial examination of the  $Fr$ , a steady increase was observed in configuration of the asymmetric hulls facing inward before rising significantly from  $Fr = 0.65$  to the peak point. However, in the configuration of asymmetric hulls facing outward, their trends rose sharply and reached a low peak point prior to a gradual increase between  $Fr = 0.58$  and  $Fr = 0.84$ , and they rose again rapidly until the true peak point.

Subsequent to their peak, each hull declined until the end of the investigated  $Fr$ ; a continuous decline was predicted. These typical trends might indicate that a hump phenomenon occurred on the peak point as it failed to occur on the non-interference pentamaran.

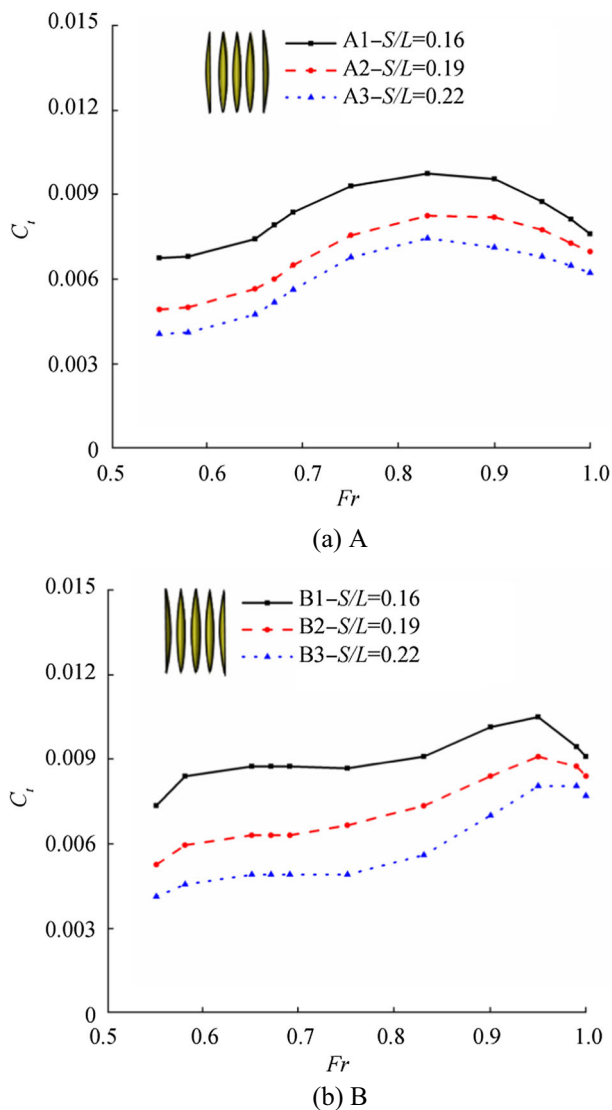


**Fig. 9** a, b Total resistance coefficient of asymmetric hull outer configuration

In addition to the above results, the findings on separation effects of the total resistance characteristics were observed at the examined  $Fr$  range and were anticipated in support of the deduction made during a previous experiment conducted in ITTC member laboratory (Yanuar et al., 2017a). From the figure, the effect of sidehull separation could not be neglected at the medium range up to the high range of  $Fr$ , whereas the effect gradually diminished near the critical  $Fr$ . The narrower hull separation might create a higher system of waves; these waves then created a higher peak as evidence of hump phenomenon, which can be proven by their IF.

Figure 10 displays the  $C_t$  curves of asymmetric hull configurations with three variations of hull separation, that is, asymmetric hulls as inner sidehulls (C and D). Their general trends were almost as similar as the asymmetric hull outer configurations, but in detail, they bore distinctive characteristics. The inboard configurations

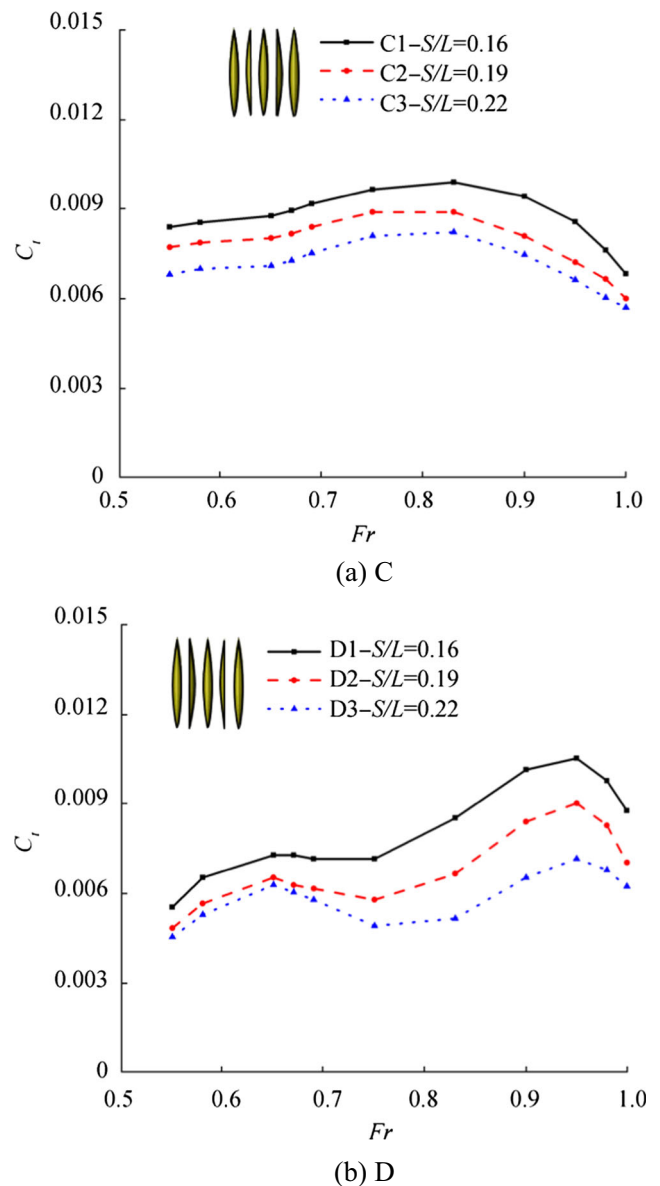


**Fig. 10** Total resistance coefficient of asymmetric-hull-inner configuration

generated one peak; the outboard configuration generated two peaks, where the first was almost flat similar to the outer outboard configuration.

From the initial  $Fr$ , the inboard configuration remained stable and climbed steadily at  $Fr = 0.65$ . Meanwhile, at the same  $Fr$ , the outboard configuration reached its first peak point (low peak). The inboard configuration reached a peak point and the outboard configuration its second peak point (true peak) at the same outer inboard and outer outboard configurations, respectively. Upon entering the critical  $Fr$ , they dropped dramatically, in which the inboard configurations dropped below their initial magnitude. Similar to the two previous configurations, they were predicted to present a continuous decline.

The effect of separation was nearly identical to the previous two conditions, with the exception of outboard configurations from the medium (initial) to high range of  $Fr$ , which is practically negligible. The phenomena on the asymmetric hull configurations were comparable with the trends of the experimental asymmetric hull pentamaran model by Yanuar et al. (2017b).

Figure 11 displays the  $C_t$  curves of symmetric hull configurations with three varied hull separations. After their slight increase at the end of the medium  $Fr$  range, the curves steadily decreased slightly until inception of the critical range. Unlike the asymmetric hull configurations, the curves undulated throughout the range. However, their decrease at the end almost plateaued, considering that they started with high  $C_t$  (in magnitude) as much the same as the inboard configurations. The effect of hull separation was also observed in the entire  $Fr$ , that is, a narrower distance created a larger magnitude.

Overall, the inboard configurations demonstrated a peak at the same  $Fr$  and were predicted to establish a hollow phenomenon after the end of the investigated  $Fr$ . Meanwhile, the outboard configurations attained a low peak and a true peak almost at the same  $Fr$ , in which the second one was much higher (in magnitude) and was predicted to establish a hollow phenomenon before the initial measurement and after the critical  $Fr$ .

### 3.3 IF

Figure 12 demonstrates the IF of all configurations. In general, the trends rose from medium  $Fr$  range to their peak at high  $Fr$  range and subsequently declined until the critical  $Fr$ , at which the values were predicted to continuously decrease. As the  $C_t$  of specific configurations was lower than that of non-interfere pentamaran, the magnitude of their IF was in a negative range;

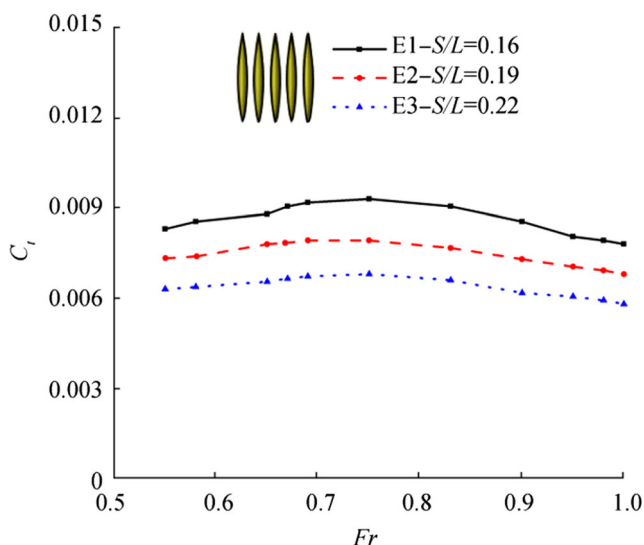


Fig. 11 Total resistance coefficient of symmetric hull configuration

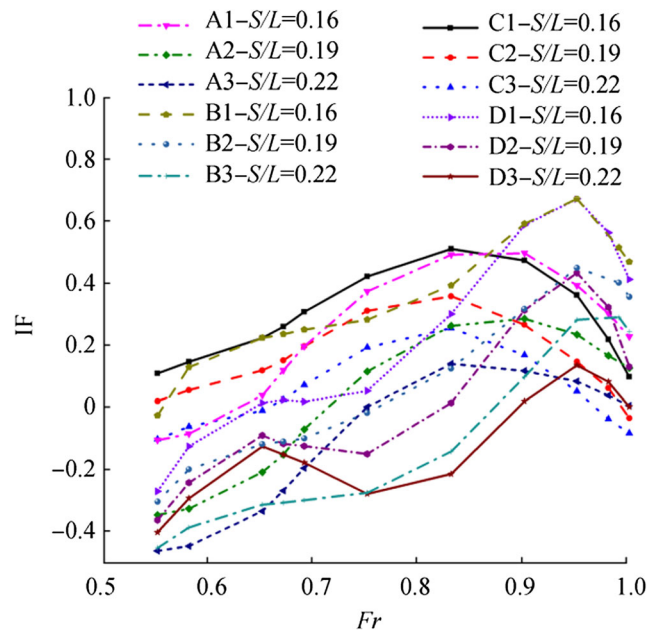


Fig. 12 IF of asymmetric hull configurations

this minimum IF (in magnitude) is a desired characteristic. However, compared with each other, not a single configuration attained the best characteristic throughout the entire range of the investigated  $Fr$ .

Furthermore, the wider hull separation expectedly generated lower IF (in magnitude) in the same configuration; these results were compared with the asymmetric hull configuration in Fig. 13.

From the figure, the asymmetric hull configuration achieved a better IF (most of them were in the negative range) than the symmetries from the medium to initially high range of  $Fr$ . After such range, the asymmetric hull configurations soared due to the hump phenomenon (and the second hump),

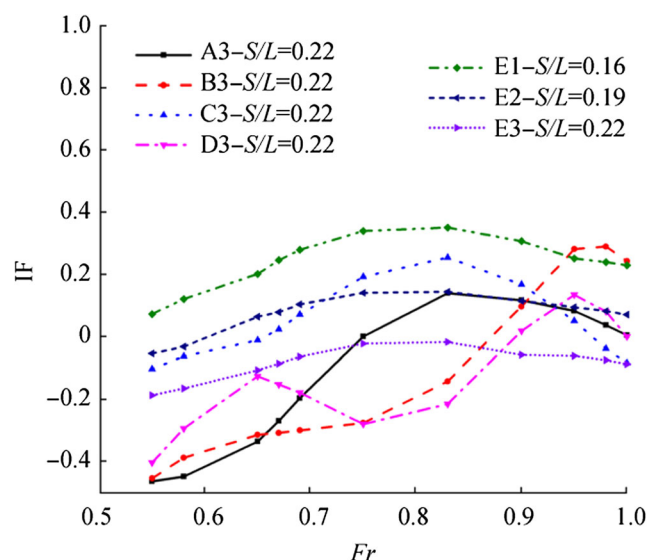


Fig. 13 IF of the symmetric and asymmetric hull configurations with  $S/L = 0.22$



thus rendering the symmetries with a desirable characteristic until the critical  $Fr$  for the same separation. Nevertheless, these compared trends of the symmetries are believed to return to normal as the trends of asymmetries were predicted to decline after the critical  $Fr$ .

Trends in IF of both asymmetric and symmetric hull configurations were almost similar to their total resistance coefficient because the  $C_t$  trends of individual hulls dropped steadily from the medium to critical  $Fr$ , resulting in similar trends in the resistance characteristics of non-interference pentamaran.

The negative IF was possibly caused by destructive interference between the systems of waves produced by individual hulls; this hollow phenomenon was indicated in the medium to high  $Fr$  range in most of the asymmetric hull configurations (excluding configuration C). However, a hump phenomenon was observed afterward, also proving that the peak (and also the second peak of outboard configurations) of their total resistance coefficient is part of the constructive interference.

In summary, all configurations created observable interference phenomena although neither fluctuating hump nor hollow phenomenon was observed in the symmetric hull configuration over the  $Fr$  range. Nonetheless, a symmetric hull configuration with the broadest separation ( $S/L = 0.22$ ) generated a constant destructive interference. Hence, its IF stayed in the negative range throughout the examined  $Fr$ ; this configuration is the only one that achieved such characteristic. Moreover, three remarkable configurations were deduced as the optimum pentamaran model depending on the  $Fr$  range; these configurations were A3, B3, and E3 at  $Fr$  ranging from the start to 0.65, from 0.65 to 0.87, and from 0.87 to the end, respectively.

## 4 Conclusion

We investigated the total resistance and interference characteristics of symmetric and asymmetric hull configurations of unstaggered Wigley hull pentamaran model in a fixed condition at medium to high  $Fr$  range. The total resistance coefficient of asymmetric hull inboard and outboard configurations produced one and two peaks, respectively. Based on the IF, these peaks, other than the first one of outboard configurations, may be caused by the constructive interference of individual hull resultant systems of waves. Constructive and destructive interferences were observed in three separation variations of the symmetric hull configuration, but they almost stabilized.

This investigation demonstrated the characteristics of total resistance and interference of the unstaggered pentamaran model using straight and detailed results. Although each configuration attained its particular resistance and interference characteristic where not a single configuration outperformed the others for the entire  $Fr$  range, three notable configurations were identified as the optimum body. These configurations

include A3, B3, and E3 at  $Fr$  ranging from the initial value to 0.65, from 0.65 to 0.87, and from 0.87 to the critical point, respectively. The asymmetric hull configuration with  $S/L = 0.22$  could generate a constant destructive interference throughout the examined  $Fr$ , whereas all other configurations could not.

Although the study found evidence of constructive interference in the high  $Fr$  range and destructive interference from medium to high  $Fr$  range, from the data collected, whether the destructive phenomenon occurs before and after the investigated  $Fr$  can possibly determine. Further studies, however, are necessary to confirm this prediction, especially at low  $Fr$  range. The use of capacity probes for wave elevation measurements on further studies might be useful to strengthen the interference results.

**Acknowledgments** The authors would like to express their sincere gratitude to all reviewers of this paper and the experts for their valuable evaluation and correction. The authors also extend their sincere gratitude to many people for their valuable contributions.

**Funding Information** This work is financially supported by the Hibah Q1Q2: NKB-0329/UN2.R3.1/HKp.05.00/2019

## References

- Brogia R, Jacob B, Zaghi S, Stern F, Olivieri A (2014) Experimental investigation of interference effects for high-speed catamarans. *Ocean Engineering* 76:75–85. <https://doi.org/10.1016/j.oceaneng.2013.12.003>
- ITTC (2002) ITTC Recommended Procedures and Guidelines: testing and extrapolation methods, resistance, uncertainty analysis, example for resistance test. Specialist Committee of 23rd ITTC: Procedures for resistance, propulsion and propeller open water tests, Vienna, Austria.
- ITTC (2011) ITTC Recommended Procedures and Guidelines: resistance test. 26th ITTC Resistance Committee, Hamburg, Germany.
- Davidson K (1942) Principles of naval architecture Vol. II, Chap. 5 Resistance and powering. The Society of Naval Architecture and Marine Engineering, Jersey City, pp 94–96
- Doctors LJ, Scrase RJ (2003) The optimisation of trimaran sidehull position for minimum resistance. The Seventh International Conference On Fast Sea Transportation, Naples, pp 1–12
- Dudson E, Gee N (2001) Optimization of the sea keeping and performance of a 40 knot pentamaran container vessel. 6th International Conference on Fast Sea Transportation, Southampton, pp 1225–1234
- Hafez K, El-Kot AR (2011) Comparative analysis of the separation variation influence on the hydrodynamic performance of a high speed trimaran. *Journal of Marine Science and Application* 10(4):377–393. <https://doi.org/10.1007/s11804-011-1083-0S>
- Hajiabadi A, Shafaghat R, Moghadam HK (2018) A study into the effect of loading conditions on the resistance of asymmetric high-speed catamaran based on experimental tests. *Alexandria Engineering Journal* 57(3):1713–1720. <https://doi.org/10.1016/j.aej.2017.03.045>
- Ikeda Y, Nakabayashi E, Ito A (2005) Concept design of a pentamaran type fast RORO ship. *Journal of the Japan Society of Naval Architects and Ocean Engineers* 1:35–42. <https://doi.org/10.2534/jjasnaoe.1.35>

- Insel M, Molland AF (1992) An investigation into the resistance components of high speed displacement catamarans. The Royal Institution of Naval Architects, London, United Kingdom Registered Charity No. 211161
- Peng H, Qin W, Hsiung CC (2004) Measuring wave resistance of high-speed multi-hull ship with a small towing tank. 27th American Towing Tank Conference, St. John's, Canada, pp 1–6
- Souto-Iglesias A, Fernández-Gutiérrez D, Pérez-Rojas L (2012) Experimental assessment of interference resistance for a Series 60 catamaran in free and fixed trim-sinkage conditions. *Ocean Engineering* 53:38–47. <https://doi.org/10.1016/j.oceaneng.2012.06.008>
- Su YM, Wang S, Shen HL, Du X (2014) Numerical and experimental analyses of hydrodynamic performance of a channel type planing trimaran. *Journal of Hydrodynamics. Ser. B* 26(4):549–557. [https://doi.org/10.1016/S1001-6058\(14\)60062-7](https://doi.org/10.1016/S1001-6058(14)60062-7)
- Tarafder MS, Ali MT, Nizam MS (2013) Numerical prediction of wave-making resistance of pentamaran in unbounded water using a surface panel method. *Procedia Engineering* 56:287–296. <https://doi.org/10.1016/j.proeng.2013.03.120>
- Tuck EO, Lazauskas L (1998) Optimum hull spacing of a family of multihulls. The University of Adelaide, Adelaide, Australia, Applied Mathematic Department, pp 1–38
- Wigley WCS, Havelock TH (1934) A comparison of experiment and calculated wave-profiles and wave resistance for a form having parabolic waterlines. *Proceedings of the Royal Society of London. Series A* 144:144–159. <https://doi.org/10.1098/rspa.1934.0039>
- Wu CS, Zhou DC, Gao L, Miao QM (2011) CFD computation of ship motions and added resistance for a high speed trimaran in regular head waves. *International Journal of Naval Architecture and Ocean Engineering* 3(1):105–110. <https://doi.org/10.2478/IJNAOE-2013-0051>
- Yanuar G, Talahatu MA, Indrawati RT, Jamaluddin A (2013) Resistance analysis of unsymmetrical trimaran model with outboard sidehulls configuration. *Journal of Marine Science and Application* 12(3): 293–297. <https://doi.org/10.1007/s11804-013-1193-y>
- Yanuar G, Muhyi A, Jamaluddin A (2016) Ship resistance of quadramaran with various hull position configurations. *Journal of Marine Science and Application* 15(1):28–32. <https://doi.org/10.1007/s11804-016-1340-3>
- Yanuar I, Faiz MH, Adib MH (2017a) Experimental analysis of diamond pentamaran model with symmetric and asymmetric hull combinations. *Journal of Engineering and Applied Sciences* 12:3433–3440. <https://doi.org/10.3923/jeasci.2017.3434.3440>
- Yanuar I, Waskito KT, Karim S, Ichsan M (2017b) Interference resistance of pentamaran ship model with asymmetric outrigger configurations. *Journal of Marine Science and Application* 16(1):42–47. <https://doi.org/10.1007/s11804-017-1401-2>
- Yu W, Chen XJ, Wu GH, Liu J, Hearn GE (2015) A fast numerical method for trimaran wave resistance prediction. *Ocean Engineering* 107:70–84. <https://doi.org/10.1016/j.oceaneng.2015.07.008>
- Zaghi S, Broglia R, Mascio AD (2011) Analysis of the interference effects for high-speed catamarans by model tests and numerical simulations. *Ocean Engineering* 38(17-18):2110–2122. <https://doi.org/10.1016/j.oceaneng.2011.09.037>